Novel Overgrowth Syndrome Phenotype Due to Recurrent De Novo *PDGFRB* Mutation

Toshiki Takenouchi, MD[1], Yu Yamaguchi, MD[1], Akiko Tanikawa, MD, PhD[2], Rika Kosaki, MD, PhD[3], Hideyuki Okano, MD, PhD[4], and Kenjiro Kosaki, MD, PhD[5]

Using exome analysis, we identified a novel overgrowth syndrome arising from a mutation in *PDGFRB*, which plays a critical role in growth and differentiation. This entity is characterized by somatic overgrowth, distinctive facial features, hyperelastic and fragile skin, white matter lesions, and neurologic deterioration. *(J Pediatr 2015;166:483-6).*

Overgrowth syndromes are characterized by an accelerated linear growth, either since the fetal period or since birth. More than 10 overgrowth syndromes have been described, and the dysregulation of signaling cascades that control cell growth and differentiation is thought to underlie these disorders.[1] Among these important signaling pathways, whether alterations in the platelet-derived growth factor–NOTCH3 signaling cascade cause a specific syndrome remains uncertain.

Patient Presentation

Patient 1 was born at 39 weeks of gestation without complications. Her birth weight was 3642 g (+1.9 SD), her length was 51.6 cm (+1.6 SD), and her head circumference was 34.6 cm (+1.1 SD). During infancy and childhood, she exhibited normal psychomotor development but had an accelerated linear growth in her height (**Figure 1**, A). At the age of 8 years, she developed a 3-cm tumor on her mandibula, which was removed surgically; the pathology was consistent with myofibroma. At the age of 14 years, her height was 182.1 cm (+4.8 SD), and her weight was 57.6 kg (+0.9 SD), her arm span was 176 cm (+3.6 SD), and her lower segment length was 91 cm (+4.6 SD). Her total hand length was 20.5 cm (+4.6 SD) and her foot length was 27 cm (+4.3 SD). Her facial features included a prominent forehead and supraorbital ridge, mild proptosis and ptosis, downslanting palpebral fissures, a wide nasal bridge, a high columella insertion, a thin upper lip, and a pointed chin. Her skin was hyperelastic, thin, and fragile (**Figure 1**, B1).

At that time, she started to exhibit recurrent episodes of depression and anxiety as well as schizophrenic symptoms, such as blocking or loosening of thought and auditory hallucinations, for which she was treated with risperidone. She had an abnormal cranial shape with protrusion of the posterior fossa and a granular pattern (**Figure 1**, C1 and D1). A fluid-attenuated inversion recovery (FLAIR) magnetic resonance imaging (MRI) of the brain showed hyperintense lesions in the white matter with no evidence of intracranial calcification on computed tomography (**Figure 1**, E1). A chest radiograph showed mild thoracic scoliosis (**Figure 1**, F1).

Patient 2 was born at term with a body weight of 2350 g (−2.1 SD), a length of 49 cm (−0.3 SD), and a head circumference of 31.5 cm (−1.5 SD). She exhibited normal psychomotor development during infancy. Blinded psychological testing using the Stanford-Binet scale (Japanese translation) indicated an IQ of 73 at the age of 5 years and 11 months. This assessment revealed that her short-term memory, in particular, was impaired. Her intellectual disability became more apparent with age, and her IQ was <40 at the age of 13 years. At the age of 17 years, her height was 164.4 cm (restricted by surgically implanted rods in her thoracic vertebrae), her lower segment length was 86 cm (+3.2 SD), her arm span was 171 cm (+2.2 SD), her hand length was 21.0 cm (+5.3 SD), and her foot length was 25.3 cm (+2.4 SD). She had distinctive facial features that were strikingly similar to those of Patient 1: a prominent forehead, proptosis, downslanting palpebral fissures, xanthoma on bilateral upper eyelids, a depressed and wide nasal bridge, thin upper lips, and a pointed chin (**Figure 1**, B2). Her skin was hyperelastic, thin, and fragile but did not have infantile myofibromatosis. She had an abnormal cranial shape with protrusion of the posterior fossa and a granular pattern (**Figure 1**, C2 and D2).

A FLAIR MRI of the brain revealed multifocal hyperintense lesions in the periventricular white matter (**Figure 1**, E2). She underwent a posterior spinal fusion for scoliosis (**Figure 1**, F2) and a secondary cranioplasty for aesthetic

FLAIR	Fluid-attenuated inversion recovery
IBGC	Idiopathic basal ganglia calcification
MRI	Magnetic resonance imaging
PDGFRB	Platelet-derived growth factor receptor B
vSMC	Vascular smooth muscle cell

From the Departments of [1]Pediatrics and [2]Dermatology, Keio University School of Medicine; [3]Division of Medical Genetics, National Center for Child Health and Development; and [4]Department of Physiology and [5]Center for Medical Genetics, Keio University School of Medicine, Tokyo, Japan

Supported by Research on Applying Health Technology (H23-013) from the Ministry of Health, Labour and Welfare, and the Leading Project for Realization of Regenerative Medicine, Support for the Core Institutes for iPS cell research from the Ministry of Education, Culture, Sports, Science, and Technology, Japan. H.O. is a scientific consultant to San Bio, Co Ltd., and Daiichi Sankyo Co, Ltd. The other authors declare no conflicts of interest.

http://dx.doi.org/10.1016/j.jpeds.2014.10.015

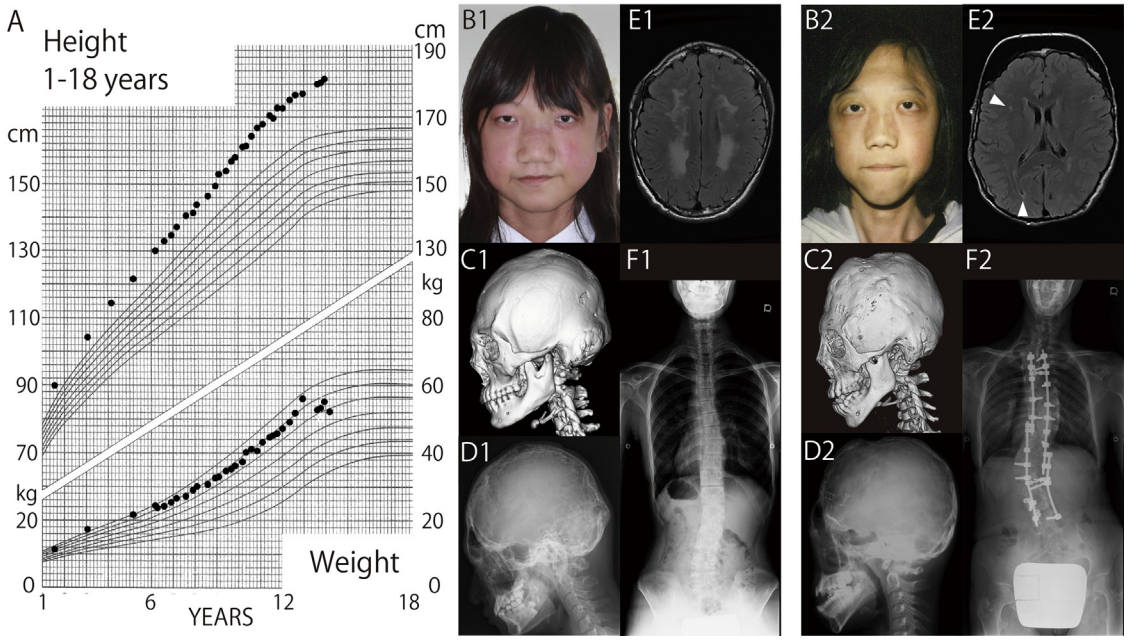

Figure 1. Clinical characteristics of the 2 patients. **A**, **B1**, **C1**, **D1**, **E1**, and **F1**, Images for Patient 1 and **B2**, **C2**, **D2**, **E2**, and **F2**, images for Patient 2 are shown. **A**, A growth chart shows accelerated linear growth for both weight and height. **B1** and **B2**, Facial photographs. **C1** and **C2**, Three-dimensional cranial computed tomography scans showing the protrusion of the posterior fossa. **D1** and **D2**, Skull radiographs showing diffuse granular patterns. **E1** and **E2**, FLAIR brain MRI results showing extensive periventricular white matter lesions (*arrowheads* in **E2**). **F1** and **F2**, Total spine radiographs showing scoliosis.

purposes at the age of 11 years. We previously reported the surgical procedure used in this patient under a presumptive diagnosis of Shprintzen-Goldberg syndrome,[2] but a subsequent mutation analysis for the causative gene, *SKI*, was negative. The family history was noncontributory in both patients (**Figure 2**).

Molecular Analysis

Informed consent from the parents and approval from the local institutional review board were obtained for the molecular studies. DNA was extracted from peripheral blood samples obtained from Patients 1 and 2 and their parents. A whole-exome analysis was performed in Family 1 via use of the MiSeq platform (Illumina, San Diego, California) and SureSelectXT Human All Exon V4 (Agilent Technologies, Santa Clara, California), which provided 10 gigabases per sample, with a mean coverage of 118-fold across the targeted coding regions. More than 98.23% of the regions were covered by >10 reads. Approximately 93 000 variants were identified in Patient 1. The sequencing reads were aligned to the reference human genome sequence (hs37d5) using Burrows-Wheeler Transform,[3] and local realignment around the indels and base quality score recalibration were performed using the Genome Analysis Toolkit[4]; duplicate reads were removed by Picard (http://picard.sourceforge.net).

Nonsynonymous coding variants, splice acceptor and donor site variants, and frameshift coding indels were filtered against dbSNP137, the 1000 Genomes Project (http://www.1000genomes.org/), ESP6500, or the Japanese SNP dataset of 1208 normal individuals (Human Genetic Variation Browser: http://www.genome.med-kyoto-u.ac.jp/SnpDB). A comparison of the exome data for Patient 1 with that of her parents and subsequent Sanger analysis retained platelet-derived growth factor receptor B (*PDGFRB*) as the sole candidate gene in an autosomal-dominant de novo model: a de novo heterozygous missense mutation in exon12 of *PDGFRB* (NM_002609), ie, c.1751C>G p.Pro584Arg, was identified in Patient 1 but not in her parents. No pathologic mutations were identified in any other genes that are associated with overgrowth syndromes, including *FBN1*, *EZH2*, *NSD1*, *PTEN*, *TGFBR1*, and *TGFBR2*. We then sequenced Family 2 and identified the same de novo mutation in Patient 2 but not in the parents (**Figure 2**). Patient 2 did not have whole-exome analysis.

Multiple prediction programs including SIFT, PolyPhen2, and MutationTaster suggested that this amino acid substitution was highly functionally relevant. An evolutional analysis showed that Pro584 and its neighboring amino acids were highly conserved across species. Pro584 is located in the juxtamembrane domain of PDGFRB, which negatively regulates the catalytic activity of cytoplasmic kinases.[5] Within the juxtamembrane domain, the Pro584 maps to the zipper or linker peptide segment, which is thought to correctly align the switching motif in the proper position when changing the autoinhibition status.[6] In addition, autophosphorylation of the neighboring